On the Vortex Dynamic of Shear-Driven Deep Cavity Flows with Asymmetrical Walls

Denis Cornu, Laurent Keirsbulck, Rogelio Chovet, Camila Chovet, Marc Lippert, Franck Kerhervé, Romain Mathis, Fethi Aloui

On the Vortex Dynamic of Shear-Driven Deep Cavity Flows with Asymmetrical Walls

D. Cornu, L. Keirsbulck, R. Chovet, C. Chovet, M. Lippert, F. Kerhervé, R. Mathis and F. Aloui

Abstract The influence of the wall asymmetry on the flow dynamics, in two-dimensional rectangular deep cavities, is studied experimentally by combining wall-pressure and PIV measurements. Main cavity flow statistics [2] have been analyzed and they have shown that the flow features are strongly affected by the asymmetry. An emphasis is given concerning the behavior of the shear-layer oscillations that are compared to the analytical deep-cavity model prediction proposed by Block (Noise response of cavities of varying dimensions at subsonic speeds. Technical Report D-8351. NASA Technical Note, 1976 [4]). The results show that, by adjusting the convection velocity, the model seems to be still able to predict the cavity self-sustained oscillations in the case of the asymmetric cavities. Stochastic estimation of the cavity flows demonstrates that convective structures are involved downstream of the cavity along the wall and highlights the physical nature of the pressure-producing flow structures.

1 Introduction

Models for understanding the unsteady features of cavity flows present a great interest for the design of large amounts of engineering applications. These models may be used to guide designs and also to enhance the feedback control performance [8]. Cavity flows are known to be potential sources of significant vibrations and other kinds of perturbations. For high subsonic Reynolds numbers, the most common mechanism of self-sustaining oscillations is the one referred to Rossiter's feedback mechanism [6]. Cavity flows are also generally classified according to their length-to-depth (L/H) and length-to-width (L/W) ratios [3] and can be qualified as deep

D. Cornu (✉) · L. Keirsbulck · R. Chovet · C. Chovet · M. Lippert · F. Aloui
LAMIH UMR 8201, 59313 Valenciennes, France
e-mail: denis.cornu@transport.alstom.com

F. Kerhervé
PPrime CNRS, UPR 3346, 86962 Chasseneuil, France

R. Mathis
LML UMR 8107, 59650 Villeneuve D'ascq, France

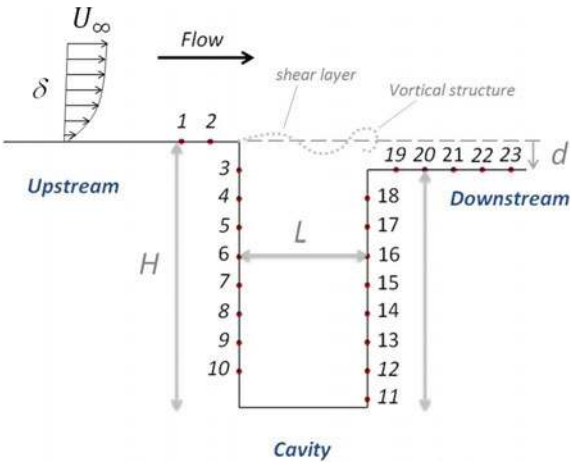

Fig. 1 Generic scheme of the cavities

if $L/H < 1$ and two-dimensional if $L/W < 1$. In literature, the cavity configuration examined is usually rectangular and symmetrical i.e. with the upstream wall-height equal to the downstream one. However, the asymmetrical cavity flow represents the geometry of numerous engineering applications such as the railway equipments encountered over the roof of many kinds of trains (Fig. 1). Such configurations are, to our knowledge, poorly described in the literature (only [1] refers to asymmetric cavity configurations). Although the classical Rossiter's mechanism seems to be very insensitive to geometrical variations due to the robustness of the self-sustained feedback mechanism, there is no information provided concerning the limitation of this model. In addition, very deep cavity configurations are also poorly documented, and the behavior of the shear layer oscillations in particular cases of deeper cavity is not clearly established up-to-now. In order to complete the knowledge regarding the canonical configuration (shallow and symmetrical) and also to prevent highly undesirable effects, the present paper studies two different asymmetrical cavity configurations and focuses on the interaction of the shear layer downstream of the cavity. The three main objectives discussed here are (i) to study the self-sustaining cavity flow oscillations, (ii) to analyze the relationship between the vortical structures and the wall-fluctuating pressure, (iii) to characterize their evolution downstream the reattachment and inside the cavity. To this aim, simultaneous PIV and wall-pressure measurements have been carried out inside and downstream the cavity. The first section of this paper presents the experimental setup and the data acquisition, the following sections deal with the wall-pressure and flow statistics, the cavity flow oscillations and the dynamical flow behavior induced by the two asymmetrical cavity flows.

2 Experimental Setup

2.1 Facility and Flow Configuration

All the experiments for this investigation were conducted in the close-loops subsonic wind tunnel facility of the LAMIH at the University of Valenciennes and Hainaut-Cambresis. The wind tunnel has a 6.25:1 contraction upstream of a 2 m wide by 2 m high by 10 m long test section. The case of asymmetrical cavity flows as illustrated in Fig. 2 is here examined. Henceforth, we used the cavity depth H (186 mm) and the upstream quantity U_∞ as the respective length and velocity scales references. The length L of the cavity was 120 mm corresponding to a Reynolds number of $Re_L = 2.4 \times 10^5$. The different studied cases are detailed in Table 1. They include positive (I), neutral (II) and negative (III) asymmetrical configurations, with a length-to-width ratio of $L/W = 0.06$ and a length-to-height ratio of $L/H = 0.6452$. Regarding the cavity flow classification, the present configuration corresponds to a "two-dimensional deep cavity". For this study, the free-stream velocity was set to 30 m/s, resulting in a Reynolds number based on the cavity height of $Re_H = 5.58 \times 10^6$ and corresponding to a Mach number of 0.088. For the flow field illustration, a Cartesian coordinate system was chosen whose streamwise origin was located at the cavity trailing edges. For all the configurations considered, the incoming boundary layer is turbulent with a thickness $\delta = 21$ mm, corresponding to a Reynolds number of $Re_\delta = 6.3 \times 10^5$.

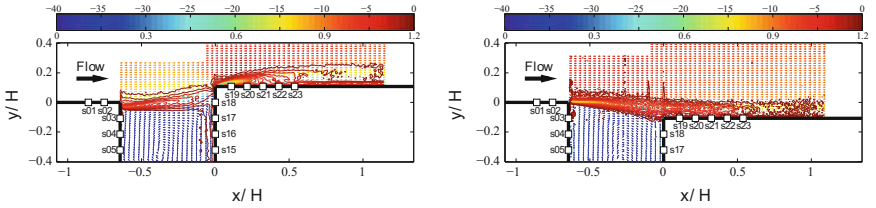

Fig. 2 Vector plots of the mean-velocity magnitude ($\|\mathbf{U}\|/U_\infty$—lower colorbar scale) and the mean-spanwise vorticity ($\Omega_z^+ = \Omega_z.H/U_\infty$—upper colorbar scale). Cases I (*left*) and III (*right*). Vector lengths are normalized in order to enhance the visibility of the flow feature inside the cavity

Table 1 Mean-cavity flow parameters

Cases	d (mm)	d/H (%)	Symbols
(I)	+20	+10.75	●
(II)	0	0.00	▲
(III)	−20	−10.75	■

2.2 Instrumentation and Data Acquisition

The various cavity flow configurations were examined in details thanks to simultaneous low-speed PIV and time-resolved pressure measurements. Two cameras were used to survey the flow inside the cavity and downstream of the trailing edge in order to examine the unsteady vortices induced by the cavity shear-layer. The PIV system included high-resolution POWERVIEW cameras with full resolution of 2048 $\times$ 2048 pixels, micro NIKKOR 50 mm lenses and a light sheet provided by a double-pulsed ND- YAG laser (QUANTEL BSLT220) operating at 532 nm which is able to produce 220 mJ per pulse. For each flow case, 2000 pairs of images are acquired with a frame rate of 7 Hz. The processing consisted of one pass with 32 $\times$ 32 pixels integration windows followed by a 16 $\times$ 16 pixels integration windows and 50% overlap. Survey of the wall-pressure is effected thanks to 23 flush mounted differential Kulite XCQ-080 sensors with pressure range of 350mBar, located before, inside and after the cavity. The distance between two sensors is constant and equal to 20 mm ($\approx 0.1H$). The pressure readings were synchronized with the PIV measurements using a TTL signal triggered by a Q-switch of the first laser cavity. Pressure signals are first low-pass filtered at 5kHz and a 12 bit A/D converter from a DEWESOFT SIRIUS- 8STG M PLUS acquisition system is used to acquire the filtered signals at a sampling frequency of 10kHz. The static pressures were also taken using pressure taps located at the same positions than that of the fluctuating sensors, and 18 additional taps stations were installed in the continuity of the downstream wall with the same spacing in order to obtain complementary information about the full recovery of the flow downstream of the cavity.

3 Effect of the Cavity Asymmetry on the Main Flow Features

3.1 Flow Statistics

Averaged PIV results are first analyzed in order to establish the main flow features and to evaluate the effect of the asymmetrical configuration upon the mean flow. For the case I, the turbulent boundary layer at the leading edge forming a shear-layer, impacts upon the cavity trailing edge and leads to the formation of a separation area onto the downstream wall. Due to local acceleration at the trailing edge, strong negative values of mean-spanwise vorticity ($\Omega_z^+ < 20$) are observed in the separation area. Moreover, high activity of vorticity is also manifest inside the cavity along the trailing side wall. This particular behavior will be discussed later. Concerning the case III, a different physical mechanism is at play. Looking at the mean-velocity magnitude distribution, the shear layer region is found to extend far downstream from the cavity trailing edge with a reattachment about $0.5H$ downstream (near sensor 23) (Fig. 3).

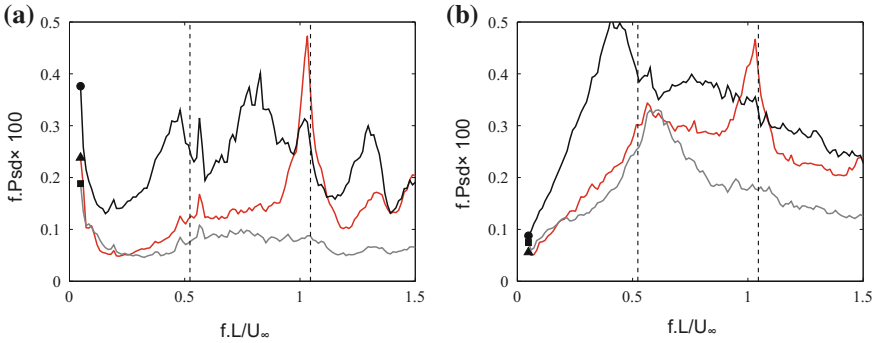

Fig. 3 Premultiplied and normalized PSD of wall-pressure fluctuations (**a**) and (**b**) the *black dashed line* shows the first and the second modes from the Block's prediction with regard to the aspect ratio ($\kappa = 0.57$)

In this case, the shear layer do not impact on the trailing edge. The concentration of substantial negative vorticity within the flow field is confined to the shear layer and especially near the leading edge of the cavity. At this location, the shear layer is very thin and the vorticity is the highest. The previously discussed vortical activity on the trailing side wall of the cavity can be detailed by the time history of the synchronous fluctuating pressure measurements for the two cases. For the case I, the footprint of the convected vortical structure involved close to the trailing side wall of the cavity (sensors 12–18) can be observed. But in the case III, we can not observe any interaction between the shear-layer and the flow inside the cavity. Results show no variation of the spatial pressure footprint on the leading side wall of the cavity. However strong fluctuations on the other side of the cavity are observed in the case I [5], compared to the other case, where any activity occurred. Downstream of the leading edge, in both cases, unsteady activity due to the separation phenomenon is also observed.

Mean and rms-values of the pressure coefficient defined along the cavity walls and obtained thanks to the static tap sensors are reported in Fig. 4 as:

$$C_p = (p - p_{ref})/(1/2\rho U_\infty^2) \text{ (with reference taken at the end of the test section)}$$

The mean-pressure distribution shows different behaviors; a classical cavity pressure profile with no significant variation is observed for the reference case II (without asymmetrical walls), a strong pressure lost occurs at the trailing edge for the case I due to the upstream flow impact previously discussed, and for the case III, a pressure increasing is clearly observed in the downstream wall region of the cavity. The rms-pressure coefficient, $C_{p\,rms} = p'_{rms}/(1/2\rho U_\infty^2)$, which essentially gives information on the unsteadiness of the flow examined, shows, only in the region of the trailing edge, significant activities for case I. Impact of shear-layer with the trailing side wall generates a separation area, thus produces an increasingly strong wall-pressure foot-

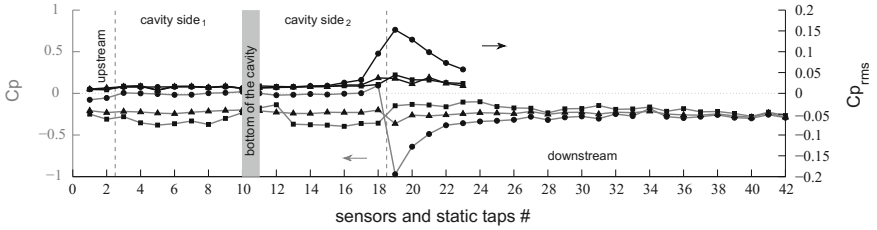

Fig. 4 Mean- and rms-pressure spatial distribution for all the studied cases. Cavity side$_1$ denotes the leading side wall of the cavity and the cavity side$_2$ refers to the other side. *Grey lines* represent C_p (refers to the *left* axis) and *black lines* represent $C_{p\ rms}$ (refers to the *right* axis)

print. The rms-pressure coefficient reaches a maximum level in the vicinity where the flow reattaches (L_R) as encountered in separated flows [10]. For case III, the wall pressure fluctuations are predominantly associated with footprints of growing shear-layer convective vortical structures moving closer to the wall.

4 Concluding Remarks

This paper is focused on adjusting linear models of cavity oscillations that are useful for feedback control purposes in the case of asymmetric cavity walls. Two typical behaviors based on different flow physics have been observed for case I and for case III. Like to the standard shear-driven deep cavity flow, a feedback mechanism between the shear layer instabilities and acoustic [9] forcing is observed in the studied asymmetrical configurations. For both cases, the classical Block's model is able to predict the cavity self-sustain oscillations by adjusting the convection velocity, although the flow dynamics are quite different. The case III shows classical shear-layer configuration with associated instability mechanism of shedding, function of the wall variation d, observed downstream the cavity trailing edge. The case I associated to a raise of the downstream cavity wall exhibits a more complex flow feature, a separate area is observed and interacts with shear-layer vortices that involves downstream of the cavity along the wall. This interaction could be a source of strong non-linear pressure-producing flow structures phenomena highlighted thanks to the stochastic analysis of the flow fields.

References

1. Yamamoto H, Seki N, Fukusako S (1983) Forced convection heat transfer on a heated bottom surface of cavity with different wall-height. Warme und Stoffubertragung 17:73–83
2. Adrian RJ, Moin P (1988) Stochastic estimation of organized turbulent structure-homogeneous shear-flow. J Fluid Mech 190:531–559

3. Larchevêque L, Sagaut P, Mary I, Labbé O, Comte P (2003) Large-eddy simulation of a compressible flow past a deep cavity. Phys Fluids 15:193–210
4. Block PJW (1976) Noise response of cavities of varying dimensions at subsonic speeds. Technical Report D-8351. NASA Technical Note
5. Block PJW (1977) Measurements of the tonal component with theory. NASA Technical Paper 1013
6. Rossiter JE (1964) Wind-tunnel experiments on the flow over rectangular cavities at subsonic and transonic speeds. Rep Aero Res Counc R M Tech
7. Rowley CW, Colonius T, Basu AJ (2002) On self-sustained oscillations in two-dimensional compressible flow over rectangular cavities. J Fluid Mech 455:315–346
8. Clarence W, Williams DR, Colonius T, Murray RM, Macmynowski DG (2006) Linear models for control of cavity flow oscillations. J Fluid Mech 547:317–330
9. El Hassan M, Labraga L, Keirsbulck L (2007) Aero-acoustic oscillations inside large deep cavities. In: 16th Australasian fluid mechanics conference, pp 421–428
10. Farabee M, Casarella MJ (1986) Measurements of fluctuating wall pressure for separated/reattached boundary layer flows. ASME J Vib Acoust Stress Reliab Des 108:301